Critical behavior of the restricted primitive model revisited

J.-M. Caillol, D. Levesque and J.-J. Weis

Laboratoire de Physique Théorique, UMR 8627, Bât. 210, Université de Paris-Sud

91405 Orsay Cedex, France

(February 1, 2008)

Abstract

Reassessment of the critical temperature and density of the restricted primitive model of an ionic fluid by Monte Carlo simulations performed for system sizes with linear dimension up to $L/\sigma = 34$ and sampling of $\sim 10^9$ trial moves leads to $T_c^* = 0.04917 \pm 0.00002$ and $\rho_c^* = 0.080 \pm 0.005$. Finite size scaling analysis based in the Bruce-Wilding procedure gives critical exponents in agreement with those of the 3d Ising universality class. An analysis similar to that proposed by Orkoulas *et al* [Phys. Rev. E **63**, 051507 (2001)], not relying on an *a priori* knowledge of the universality class, leads to an unaccurate estimate of T_c^* and to unexpected behavior of the specific heat and value of the critical exponent ratio γ/ν.

I. INTRODUCTION

Despite endeavor over more than a decade to elucidate the nature of the critical behavior of the restricted primitive model (RPM) for ionic fluids, prototype of a system governed by long range Coulomb interactions, no unassailable answer to this question has yet been provided by theory, experiment or computer simulation[1–6]. The long range character of the interaction would suggest classical (mean field) behavior, whereas the well known screening of the interactions pleads in favor of an Ising-type criticality typical of systems with short range interactions. In contrast to the latter case a rigorous renormalization group (RG) treatment allowing to decide in favor of one or the other universality class is, for the moment, still unavailable due to the lack of a satisfactory mean field starting point for RG analysis[7,8].

On the experimental side[6] an indisputable interpretation of criticality in ionic systems and assessment of the role played by the Coulomb interaction is somewhat hampered by the possible interplay of the Coulomb interaction with other forces driving phase separation (as, for instance, solvophobic effects), uncertainties of measurement close to the critical point or choice of appropriate order parameter to analyse the results. It seems however well established now that for many experimental systems apparent mean field behavior applies with sharp crossover (much sharper than in non-ionic fluids) to Ising criticality close to the critical temperature[6].

Computer simulations can isolate the effect of the Coulomb interactions but are plagued with their own difficulties when approaching the critical region, in particular by the limited system sizes that are currently accessible for off-lattice systems. Finite size corrections to the scaling behavior may therefore be important and thwart extrapolation to the thermodynamic limit. In addition, the fact that the RPM, as well as most realistic continuum models, lack symmetries, that are present, for instance, in the Ising or lattice-gas models has the consequence that the asymptotic scaling properties are more complex than for the latter systems.

Starting with the seminal work of Bruce and Wilding (BW)[9,10] simulation results for the

critical behavior of asymmetric fluids have customarily been analyzed along the lines of the revised scaling theory of Rehr and Mermin[11] in which the two relevant scaling fields h (the strong ordering field) and τ (the weak thermal field) are assumed to be linear combinations of deviations from the critical values of the chemical potential μ and the inverse temperature $\beta = \frac{1}{kT}$ (for the definition of the reduced quantities see below)

$$h = \mu^* - \mu_c^* + r(\beta_c^* - \beta^*) \tag{1}$$

$$\tau = \beta_c^* - \beta^* + s(\mu^* - \mu_c^*) \tag{2}$$

where s and r are system dependent coefficients defined in Ref. 11. The revised scaling theory assumes analyticity of $\mu(T)$ at the critical temperature T_c. Although this is the case for the Ising model and some models with "hidden" symmetry, there is no compelling reason that, in general, for fluid systems $\mu(T)$ should lack a singularity as recognized already by Rehr and Mermin[11], Yang and Yang[12] and emphasized more recently by Fisher and coworkers[13–15]. The latter authors, by carefully analyzing experimental results for the constant volume heat capacity

$$C_V(T) = VT(\partial^2 p/\partial T^2)_V - NT(\partial^2 \mu/\partial T^2)_V \tag{3}$$

$$= C_p + C_\mu \tag{4}$$

give evidence for a divergence of $(\partial^2\mu/\partial T^2)_V$, the so called Yang-Yang (Y-Y) anomaly[12], in CO_2 and propane when approaching the critical point from below, e.g. along the critical isochore[13,14]. According to Fisher and Orkoulas, in order to accomodate the Y-Y anomaly, the pressure should combine with β and μ in Eqs. 1 and 2 [13]. This in turn will affect the finite size scaling (f.s.s.) analysis - at the core of all simulation studies - through appearance of additional size dependent terms which may compete with those of the customary description. One can note, however, that for a hard core square-well model fluid the strength of the Y-Y anomaly appears to be quite small[15].

The present study was undertaken to extend simulation work on the RPM[16,17] to system sizes larger than previously considered, covering the volume range $(5000 - 40000)\sigma^3$ (or

linear dimension $L = 17 - 34\sigma$), thus providing a valuable check of the validity of previous extrapolations of the critical parameters to their thermodynamic limit. By the same token statistics of the runs performed previously with the smaller system sizes were considerably increased. In addition, these new simulations gave us the opportunity to investigate the behavior of the two contributions C_p and C_μ to the specific heat near its critical point. The occurrence of a divergent C_μ would call for a revision of the revised scaling assumptions of Rehr and Mermin[11] as pointed out by Fisher and Orkoulas[13].

The model and a few computational details are given in Sec. II and the results in Sec. III. The conclusions are summarized in Sec. IV.

II. MODEL AND BOUNDARY CONDITIONS

In the RPM of an ionic solution $N/2$ particles carrying a charge $+q$ and an equal number of particles with charge $-q$ interact via a hard sphere excluded volume and a Coulomb interaction, i.e.

$$v_{ij}(r) = \begin{cases} +\infty & r \leq \sigma \\ \dfrac{q_i q_j}{D}\dfrac{1}{r} & r > \sigma \end{cases} \tag{5}$$

where σ is the hard sphere diameter and D the dielectric constant of the solvent assumed to be a dielectric continuum.

In fact a thermodynamic state is specified by the combination $T^* = \dfrac{kTD\sigma}{q^2}$ defining a reduced temperature (or its inverse $\beta^* = 1/T^*$) and a reduced chemical potential $\mu^* = \mu/kT - 3\ln(\Lambda/\sigma)$ (k Boltzmann's constant, Λ the de Broglie thermal wavelength). A reduced density is defined as $\rho^* = N\sigma^3/V$ (N total number of ions, V volume).

When hyperspherical boundary conditions[18] are used, as done here in accord with our previous work[16,17], the particles are confined to the surface S_3 of a hypersphere in 4d space. In this geometry the RPM may be viewed as a system of identical particles of charge q (bicharges) interacting by the potential[18]

$$v_{ij}^{el,S_3} = \frac{q^2}{R}\cot\psi_{ij} \ (0 < \psi_{ij} < \pi). \tag{6}$$

The distance r_{ij} between two particles on S_3, measured along the geodesic joining them, is related to the angle ψ_{ij} by $r_{ij} = R\psi_{ij}$ where R is the radius of the hypersphere. The Monte Carlo (MC) simulations were performed in the grand canonical (GC) ensemble using a biasing scheme[17,19] to enhance the acceptance ratio of the trial insertion and deletion moves. During the simulation runs we recorded, at fixed μ, T and V the joint distribution $p_L(\rho, u)$ of particle number and energy density $u = U/V$ which is the basic ingredient for our analysis of the critical properties. Use of histogram reweighting[20] was made to infer the distribution at a state (β, μ) from the known one at a nearby state (β_0, μ_0).

III. RESULTS

In this section we intend to reassert, within the mixed-field f.s.s. approach of Bruce and Wilding[10] , our previous estimates[17] of the critical parameters taking into account new simulations at volumes $V/\sigma^3 = 20000$ and 40000 and results with increased statistics at $V/\sigma^3 = 5000$ and 10000. Briefly stated, in this approach the appropriate scaling operators conjugate to the scaling fields h and τ (Eqs 1 and 2) are assumed to be

$$\delta\mathcal{M} = \mathcal{M} - < \mathcal{M} >_c \tag{7}$$

$$\delta\mathcal{E} = \mathcal{E} - < \mathcal{E} >_c \tag{8}$$

where

$$\mathcal{M} \;=\; \frac{\rho - su}{1 - sr} \tag{9}$$

$$\mathcal{E} \;=\; \frac{u - r\rho}{1 - sr} \tag{10}$$

and $< \mathcal{M} >_c$ and $< \mathcal{E} >_c$ are the values at criticality.

With this postulate the critical behavior of the fluid system can be mapped on that of the (symmetric) Ising spin system. In particular, the distribution $p_L(\mathcal{M})$ of the ordering parameter should be invariant under the symmetry transformation $\delta\mathcal{M} \to -\delta\mathcal{M}$ along the

coexistence curve $h = 0$ and similar to that of the 3d Ising magnetization. The strategy offered by Bruce and Wilding[10] to determine the critical parameters T_c and ρ_c is to vary μ, T and s until the distribution $p_L(\mathcal{M})$ derived from $p_L(\rho, u)$ (measured in the simulation) through the linear transformations Eqs. 9 and 10 and integration over $\mathcal{E}$ matches the distribution of the 3d Ising universality class p^*_{is} known from lattice spin simulations[21,22].

Due to the finite size of the simulation volumes the critical parameters so obtained will be shifted with respect to their infinite volume values. Finite size scaling theory tells us, however, how the apparent parameters scale with system size L. The critical temperature, for instance, should vary as

$$T^*_c(L) - T^*_c(\infty) \propto L^{-1/\nu-\theta/\nu} \tag{11}$$

where allowance has been made for correction to scaling through the Wegner exponent θ[23].

The thermodynamic states at which histograms were recorded are summarized in Table I. All simulation runs, including those at $V/\sigma^3 = 5000$ and 10000 are new. The total number of selected configurations, spaced by 250 MC trial moves, varies between 10^8 and $4\ 10^8$ depending on volume (cf. Table I) and is thus 4-10 times larger than that generated in Ref. 17. By histogram reweighting we estimated, for each volume, an apparent critical temperature such that the order parameter distribution $p_L(\mathcal{M})$, normalized to have unit variance, matches the 3d Ising model universality class.

The matching of $p_L(\mathcal{M})$ and $p^*_{is}(\mathcal{M})$ at $T^*_c(\infty)$ was realized in Ref. 17 using the estimate of $p^*_{is}(\mathcal{M})$ made by Hilfer and Wilding[21] for the 3d Ising model on cubic lattices of sizes 20^3 and 30^3. Recently two new estimates of $p^*_{is}(\mathcal{M})$ have been obtained by Tsypin and Blöte[22] for the 3d Ising model and the spin-1 Blume-Capel model with lattice sizes up to 58^3. The two evaluations of $p^*_{is}(\mathcal{M})$ at $T^*_c(\infty)$ differ notably, especially for the values of the two maxima of $p^*_{is}(\mathcal{M})$ at $\mathcal{M} = \pm\mathcal{M}_{max}$. However, Tsypin and Blöte[22] consider the distribution $p^*_{is}(\mathcal{M})$ evaluated for the Blume-Capel model to be the more reliable since finite size effects appear to be smaller for the largest lattice sizes considered in their simulations. In view of these differences it seemed thus justified, in order to determine the apparent critical temperatures

$T_c^*(L)$ for the different volumes, to realize the matching of $p_L(\mathcal{M})$ using $p_{is}^*(\mathcal{M})$ obtained with the Blume-Capel model. For volume sizes $V/\sigma^3 \leq 10000$ the matching procedure is not without ambiguity due to poor or insufficient sampling of densities smaller or close to $2/V$. In order to minimize the bias on $T_c^*(L)$ introduced by insufficient sampling of the low densities the matching has been realized, for each volume, by determining the smallest mean square deviation between $p_{is}^*(\mathcal{M})$ and $p_L(\mathcal{M}, T, \mu, s)$ by minimizing

$$\chi_L^2 = \int_{-1.5}^{1.5} (p_{is}^*(x) - p_L(x, T, \mu, s))^2 dx \tag{12}$$

in the domain of values where $p_L(\mathcal{M})$ seems most reliable with the constraint that μ and s are such that $p_L(x_{max}) = p_L(-x_{max})$. Here $x = \delta\mathcal{M}/\sqrt{<\delta\mathcal{M}^2>}$

Figure 1 shows χ_L^2 as a function of s in the vicinity of $T_c^*(L)$ for the four volumes considered and $p_{is}^*(\mathcal{M})$ given by the Blume-Capel model[22]. For $V/\sigma^3 = 5000$ there are two equivalent minima at $T_c^* = 0.004934$ for $s = -1.44$ and $s = -1.45$. The latter value has been retained. A similar minimization has also been realized using $p_{is}^*(\mathcal{M})$ calculated for the 3d Ising model[22]. In this way one obtains two sets of values of $T_c^*(L)$, plotted in Fig. 2, from which $T_c^*(\infty)$ can be determined using Eq. 11 for the extrapolation of the $T_c^*(L)$ as a function of $L^{-(\theta+1)/\nu}$. These extrapolations lead to the estimates 0.04917 ± 0.00002 using $p_{is}^*(\mathcal{M})$ derived from the Blume-Capel model and 0.04916 ± 0.00002 using $p_{is}^*(\mathcal{M})$ obtained with the 3d Ising model. The errors on $T_c^*(L)$ correpond to those on the localisation of the minimum of χ_L^2. In the following $p_{is}^*(\mathcal{M})$ will refer to the universal distribution obtained from the Blume-Capel model.

Use of this new determination of $p_{is}^*(\mathcal{M})$ leads to an increase of the critical temperature T_c^* by $\sim 0.5\%$ with respect to our previous estimate[17]. It is worth noticing that the latter estimate of T_c^* included volumes $V/\sigma^3 \leq 5000$ for which the region of very low density states ($\leq 2/V$) cannot be sampled.

The collapse of $p_L(\mathcal{M})$, obtained by minimizing χ_L^2, on the universal distribution p_{is}^* for the different volumes is shown in Fig. 3 . At volume $V/\sigma^3 = 5000$ a mismatch is observed at the lowest values of $\mathcal{M}$ due, as explained in Ref. 17, to inadequate sampling of the low

density configurations at small volume. At volumes $V/\sigma^3 = 10000$ and 20000 the agreement is excellent. It is less good at the larger volume, especially for $V/\sigma^3 = 40000$. The most plausible explanation for this discrepancy is a statistical effect due to insufficient sampling of the region of densities comprised between the high and low density maxima. We attempted to improve the sampling by using a multicanonical method[10,24], which permits enhanced crossing of the free energy barrier separating the gas and liquid phases, but did not observe a sensible reduction of the discrepancy.

From the knowledge of the order parameter distribution we can calculate the ratio

$$Q_L = \frac{< \delta\mathcal{M}^2 >_L^2}{< \delta\mathcal{M}^4 >_L} \tag{13}$$

which takes a well-defined universal value Q^* at $T = T_c$ and $L \to \infty$[25,26]. From f.s.s. theory it follows that Q_L can be expanded in the vicinity of the critical point as[26]

$$\begin{aligned} Q_L(\beta^*) = Q^* + q_1(\beta^* - \beta_c^*)L^{1/\nu} + q_2(\beta^* - \beta_c^*)^2 L^{2/\nu} \\ + q_3(\beta^* - \beta_c^*)^3 L^{3/\nu} + \cdots + b_1 L^{y_i} + \cdots . \end{aligned} \tag{14}$$

where the last term takes into account contributions from irrelevant fields and q_1, q_2, q_3 and b_1 are non-universal constants. For each volume V and T in the vicinity of $T_c^*(\infty)$, Q_L has been determined by calculating the moments of the symmetrized distribution $p_L(\mathcal{M}, T)$, i.e. such that $p_L(\mathcal{M}_{max}) = p_L(-\mathcal{M}_{max})$ for an appropriate choice of μ^*, s having the value corresponding to that which realizes the matching of $p_L(\mathcal{M})$ at $T_c^*(\infty)$ since, as apparent from Fig. 1, s depends weakly on T at given volume.

A fit of $Q_L(\beta^*)$ obtained for the four volumes along the coexistence curve turned out not to be possible, within the present precision of data, when β_c^*, Q^*, q_1, q_2, q_3, b_1 and the exponents ν, θ and y_i were all considered as free parameters. In contrast, when fixing β_c^* to the value derived above, $\beta_c^* = 1/0.04917$, and using the value $y_i = -\theta/\nu = -0.84$ a fit better than 1% is obtained giving $Q^* \approx 0.63 \pm 0.01$ and $\nu = 0.66 \pm 0.03$. Conversely, if Q^* is fixed at the universal value of the Ising class and $\theta = 0.53$, all other parameters being left free, one obtaines $T_c^* = 0.04918$ and $\nu = 0.63$. These values of Q^* and ν are close to those of the 3d Ising universality class 0.623 [26] and 0.630 [27], respectively.

The variation of Q_L as a function of β^* for the different volumes is shown in Fig. 4. Although there is considerable spread in the intersection points due to correction-to-scaling contributions, the corresponding values of Q^* are close to the Ising value (0.623) and beyond doubt permit to rule out mean field behavior ($Q^* = 0.457$)[28]. Further support for Ising-like exponents is provided by the scaling of $< \delta\mathcal{M}^2 >$ at $T_c^*(L)$ versus $L^{2\beta/\nu}$ [25] yielding $\beta/\nu = 0.52$ in accord with the 3d Ising value (0.517) and in clear contrast with the classical value 1 (cf. Fig. 5).

The ordering operator distribution $p_L(\mathcal{M})$ at $T_c^*(\infty) = 0.04917$ is shown in Fig. 6 for the different volumes considered. Due to the higher value of the critical temperature compared to that estimated in Ref. 17 (0.0488) the $p_L(\mathcal{M})$ are much closer to the infinite system limit than those of Ref. 17.

Extrapolation of the apparent chemical potentials defined as $\mu_c^*(L) \equiv \mu^*(\beta_c^*(L), L)$ using a relation similar to Eq. 11, yields the infinite volume critical chemical potential $\mu_c^* = -13.600 \pm 0.005$. Finally, an apparent critical density $\rho_c^*(L)$ was obtained from $\int d\rho\ \rho p_L(\rho)$ calculated at $\beta_c^*(L)$ and $\mu_c^*(L)$. As already remarked in Refs. 17 and 29 the results are nearly constant within statistical error extrapolating to the infinite volume critical density $\rho_c^* = 0.080 \pm 0.005$. The critical density remains thus unchanged from our previous estimate[17].

The scaled distributions p_L^ρ associated with those of $p_L(\mathcal{M})$ obtained at $T_c^*(\infty)$ (cf. Fig. 3) are shown in Fig. 7. With increasing system size a net tendency manifests for a more symmetric curve with equal peak heights as expected in the limit $L \to \infty$. However, an increase of the statistical error with volume is also apparent as well as the inedequate sampling at low density.

In summary, reanalysis, in the framework of the scheme of Bruce and Wilding[9,10], of new simulation results involving four times larger volumes than considered in previous work, increased statistics and use of a recent determination of the order parameter distribution of the 3d Ising universality class[22] leads to i) a change of critical temperature of 0.5 %. ii) an estimate of the critical exponents ν and β/ν and the parameter Q^* based on the sole knowledge of the critical temperature and parameter θ in contrast with our previous results

which were shown to be only compatible with the Ising universality class. These new data confirm our previous conclusion of the agreement of the critical behavior of the RPM with that of the 3d Ising system.

In order to avoid an *a priori* assumption of the universality class, Orkoulas *et al* [15] propose to study the scaling properties of moments or combination of moments, $Y_j(\rho, T; L)$, of the distribution $p_L(\rho, u)$ as, for instance, the specific heat or the susceptibility $Y_7 = \frac{1}{V}[< O^2 > - < |O| >^2]$ ($O = N - < N >$), computed as a function of temperature along an appropriate locus in the (T, ρ) plane. Extrapolation to the thermodynamic limit of the effective temperatures associated with the peak positions in Y_j for each system size provides estimates of $T_c(\infty)$ and critical exponents. We have applied this analysis to the RPM for all the functions displayed in Ref. 15 choosing as locus the line of inflection points of the density versus chemical potential along an isotherm (the $\chi_{NNN} =< O^3 > /V = 0$ locus of Ref. 15). The variation of $T_c^*(L)$ associated with the peak positions of the functions C_V, Y_3, Y_7, Y_{8-}, Y_{8+} and Y_{12}, defined in Ref. 15, along the locus $\chi_{NNN} = 0$ is shown in Fig. 8 as a function of $L^{-1/\nu}$. Although all functions seem to vary nearly linearly the extrapolated critical temperatures present a rather large scatter between 0.0493 and 0.0490. Only those associated with Y_7 and Y_{8+} are compatible with the critical temperature 0.04917 derived from the BW f.s.s. procedure. It is worth noticing that the statistical error on the values of Y_j is difficult to estimate but a 1% value seems to be a conservative lower bound.

An alternative approach we propose is to search for a remarkable point (saddle point or extremum) of Y_j in the whole (ρ, T) plane and measure its height as a function of volume. Provided such a remarkable point exists and is located in the estimated critical region, the height of Y_j should scale as $L^{\omega/\nu}$ where ω is the exponent of the power-law type divergence of Y_j in the thermodynamic limit.

All functions Y_j depending explicitly on the absolute value of O considered in Ref. 15 (as, for instance, Y_3, Y_7, Y_8 ...) were found to exhibit remarkable points in the critical region. As an example we considered the function Y_7 which gave the best estimate for T_c^* (cf. Fig. 8). Figure 9 shows the saddle point present in Y_7. A linear fit of the logarithm of the value

of Y_7 at the saddle point versus $\ln L$, shown in Fig. 10, yields $\gamma/\nu = 1.89 \pm 0.03$. We stress that the mentioned error is the error on the slope inferred from the linear regression; this error should not be assimilated with the statistical error on γ/ν which results from the error on the estimates of the histograms used to calculate Y_7 and is beyond reach. The value of γ/ν found is notably lower than the 3d Ising value (1.967) [27] or the mean field value (2.0). This rather surprising result can be considered as significant only when a reliable estimate of the statistical error on γ/ν is available.

On the other hand functions involving O show remarkable points the value of which should scale as $L^{n\beta/\nu}$. Unfortunately, no sufficiently precise numerical location of these points could be achieved and therefore they could not be used to estimate β/ν.

Finally, the specific heat at constant volume C_V/V, calculated along the locus $\chi_{NNN} = 0$ [15] is shown in Fig. 11. Although the peak positions shift correctly towards the critical temperature determined above and the widths of the curves narrow with increasing system size, there is no detectable scaling of the amplitudes of the peaks over the volume range considered in this work. Similar conclusions are reached for the chemical potential term C_μ/V of the specific heat (cf. Eq. 4) as evidenced in Fig. 11. A possible explanation for the non-singular behavior of C_V is that the amplitude of the singular term in C_V is small in the RPM and the specific heat dominated by its regular contribution, It can also be remarked that the peak heights in C_V/V would scale, assuming Ising value for the specific heat exponent, only by a factor $2^{\alpha/\nu} \sim 1.12$ when doubling the linear dimensions of the system. It is quite possible that such a small increase of peak height is not observable within the statistical uncertainty of our calculations. Results for the isochoric specific heat of the discrete lattice RPM[30] show a much more pronounced enhancement of the maximum of C_V with system size.

IV. CONCLUSION

New MC simulations for system sizes up to $L/\sigma = 34$, analyzed within the context of the revised scaling theory[10,11] lead to a new estimate of T_c^* for the RPM, differing by 0.5 % from our earlier one[17], and to critical exponents ν and β/ν and value of Q^* in excellent agreement with those of the 3d Ising universality class. This estimate relies on matching the order parameter distribution of the Blume-Capel model obtained recently in lattice simulations by Tsypin and Blöte[22]. An analysis based on the moments of Y_j which makes no assumption of the universality class failed to give a precise estimate of T_c^*. Furthermore, the value of γ/ν estimated from the critical behavior of Y_7 does neither match the Ising nor the mean field value. The behavior of the constant volume specific heat gives no indication of the expected $L^{\alpha/\nu}$ scaling within the range of system sizes considered. In addition, the contribution C_μ to the specific heat does not show any anomaly which would challenge the use of Eqs. 1 and 2 for the scaling fields[13]. Recent studies of a discrete version of the RPM, with lattice sizes up to $L = 22$, based on a finite size scaling analysis similar to the one considered in this work[31] or on the methodology proposed in Ref. 15 [32] also conclude to Ising criticality of the RPM.

ACKNOWLEDGMENTS

We thank the referee for valuable comments on the manuscript. Computing time on the NEC SX-5 was granted by the Institut de Développement et de Ressources en Informatique (IDRIS).

REFERENCES

[1] M.E. Fisher, J. Stat. Phys. **75**, 1 (1994).

[2] G. Stell, J. Stat. Phys. **78**, 197 (1995).

[3] M.E. Fisher, J. Phys.: Condens. Matter **8**, 9103 (1996).

[4] G. Stell, J. Phys.: Condens. Matter **8**, 9329 (1996).

[5] G. Stell, in *New Approaches to Problems in Liquid State Theory*, NATO Science Series C Vol. 529, edited by C. Caccamo, J.-P. Hansen and G. Stell (Kluwer Academic, Dordrecht, 1999).

[6] H. Weingärtner and W. Schröer, Adv. Chem. Phys. **116**, 1 (2001).

[7] A.G. Moreira, M.M. Telo da Gama and M. E. Fisher, J. Chem. Phys. **110**, 10058 (1999).

[8] A. Ciach and G. Stell, J. Mol. Liq. **87**, 255 (2000).

[9] A.D. Bruce and N.B. Wilding, Phys. Rev. Lett. **68**, 193 (1992).

[10] N.B. Wilding and A.D. Bruce, J. Phys.: Condens. Matter **4**, 3087 (1992).

[11] J.J. Rehr and N.D. Mermin, Phys. Rev. A **8**, 472 (1973).

[12] C.N. Yang and C.P. Yang, Phys. Rev. Lett. **13**, 303 (1964).

[13] M. E. Fisher and G. Orkoulas, Phys. Rev. Lett. **85**, 696 (2000).

[14] G. Orkoulas, M. E. Fisher and C. Üstün, J. Chem. Phys. **113**, 7530 (2000).

[15] G. Orkoulas, M. E. Fisher, and A. Z. Panagiotopoulos, Phys. Rev. E **63**, 051507 (2001).

[16] J.M. Caillol, D. Levesque and J.J. Weis, Phys. Rev. Lett. **77**, 4039 (1996).

[17] J.M. Caillol, D. Levesque and J.J. Weis, J. Chem. Phys. **107**, 1565 (1997).

[18] J.M. Caillol, J. Chem. Phys. **99**, 8953 (1993).

[19] G. Orkoulas and A.Z. Panagiotopoulos, J. Chem. Phys. **101**, 1452 (1994).

[20] A.M. Ferrenberg and R.H. Swendsen, Phys. Rev. Lett. **61**, 2635 (1988); **63**, 1195 (1989).

[21] R. Hilfer and N.B. Wilding, J. Phys. A **28**, L281 (1995).

[22] M.M.. Tsypin and H.W.J. Blöte, Phys. Rev. E **62**, 73 (2000).

[23] F.G. Wegner, Phys. Rev. B **5**, 4529 (1972).

[24] B.A. Berg and T. Neuhaus, Phys. Rev. Lett. **68**, 9 (1992).

[25] K. Binder, Z. Phys. B **43**, 119 (1981).

[26] H.W.J. Blöte, E. Luijten, and J.R. Heringa, J. Phys. A: Math. Gen. **28**, 6289 (1995).

[27] R. Guida and J. Zinn-Justin J. Phys. A **31**, 8103 (1998).

[28] E. Brézin and J. Zinn-Justin, Nucl. Phys. B **257**, 867 (1985); E. Luijten and H.W.J. Blöte, Phys. Rev. Lett. **76**, 1557 (1996).

[29] G. Orkoulas and A.Z. Panagiotopoulos, J. Chem. Phys. **110**, 1581 (1999).

[30] E. Luijten, M. E. Fisher and A.Z. Panagiotopoulos, J. Chem. Phys. **114**, 5468 (2001).

[31] A.Z. Panagiotopoulos, J. Chem. Phys. **116**, 3007 (2002).

[32] E. Luijten, M. E. Fisher and A.Z. Panagiotopoulos, arXiv:cond-mat/0112388 (2001).

TABLES

TABLE I. The table summarizes, for each value of the reduced simulation volume V/σ^3, the range of temperatures T^* and chemical potentials μ^* at which simulations have been performed. n_T denotes the number of different temperatures considered and n_s the total number of thermodynamic states. The last two columns give the number n_r of configurations generated in each simulation run and n_c the total number of selected configurations (spaced by 250 trial moves) used to compute a reweighted histogram at given V.

V/σ^3	T^*	n_T	n_s	μ^*	n_r	n_c
5000	0.04928	1	1	-13.569	$23\,10^9$	$92\,10^6$
10000	0.04915	1	2	-13.603 to -13.605	$15\,10^9$	$120\,10^6$
20000	0.0489 – 0.04920	4	4	-13.59 to -13.65	$87\,10^8$	$153\,10^6$
40000	0.04910 – 0.04931	6	14	-13.56 to -13.62	$62\,10^8$	$390\,10^6$

FIGURES

FIG. 1. χ^2_L (Eq. 12) as a function of s for the four volumes considered. For each volume, five temperatures are shown differing by 0.00001. The lowest temperatures are 0.04920 (V/σ^3=40000), 0.04919 (V/σ^3=20000), 0.04923 (V/σ^3=10000), 0.04933 (V/σ^3=5000) and the corresponding curves are marked by circles. Those corresponding to temperatures successively increased by 0.00001 are marked as squares, diamonds, up triangles and left triangles, respectively.

FIG. 2. The apparent critical temperature $T_c^*(L)$ as a function of $L^{-(\theta+1)/\nu}$, with $\theta = 0.53$ and $\nu = 0.630$ obtained by matching the universal distribution calculated for the Blume-Capel model[22] (circles) and the 3d Ising model[22] (squares). In the former case the apparent temperatures are 0.04934, 0.04926, 0.04921 and 0.04922 for volumes V/σ^3=5000, 10000, 20000 and 40000, respectively, extrapolating by linear least square fit to the infinite volume temperature estimate $T_c^* = 0.04917 \pm 0.00002$. In the latter case the apparent temperatures are 0.04932, 0.04923, 0.04920 and 0.04921 for volumes V/σ^3=5000, 10000, 20000 and 40000, respectively, extrapolating by linear least square fit to $T_c^* = 0.04916 \pm 0.00002$. L is in units of σ.

FIG. 3. Collapse of the ordering operator distribution function $p_L(\mathcal{M})$ onto the universal Ising ordering operator distribution $p^*_{is}(x)$ for $V/\sigma^3 = 5000$, $T_c^*(L) = 0.04934$ ($s = -1.45$) , $V/\sigma^3 = 10000$, $T_c^*(L) = 0.04926$ ($s = -1.465$), $V/\sigma^3 = 20000$, $T_c^*(L) = 0.04921$ ($s = -1.47$) and $V/\sigma^3 = 40000$, $T_c^*(L) = 0.04922$ ($s = -1.43$). The universal distribution $p^*_{is}(x)$ (solid circles) is the MC result of Tsypin and Blöte[22] obtained from the Blume-Capel model. The scaling variable is $x = a_{\mathcal{M}}^{-1} L^{\beta/\nu}(\mathcal{M} - < \mathcal{M} >_c)$. Scale factors are chosen such that the distributions have unit variance.

FIG. 4. Variation of the ratio $Q_L = < \delta\mathcal{M}^2 >_L{}^2 / < \delta\mathcal{M}^4 >_L$ as a function of reduced inverse temperature β^* for the different volumes considered. The size of the symbols is slightly smaller than the estimated uncertainties. From top to bottom, V/σ^3=40000, 20000, 10000 and 5000, respectively. The symbols denote the simulation results and the lines the fit by means of Eq. 14.

FIG. 5. Variation of $\ln < \delta\mathcal{M}^2 >_L$ at $T_c^*(L)$ as a function of $\ln L$. Error bars are of the order of 1 %. The slope of the linear least square fit is $2\beta/\nu \approx 1.04$.

FIG. 6. Ordering operator distribution functions $p_L(x)$ at $T_c^*(\infty) = 0.04917$ and chemical potential μ^* determined such that $p_L(\mathcal{M})$ is symmetric, for $V/\sigma^3 = 5000$ (open squares), 10000 (open circles), 20000 (solid squares) and 40000 (solid circles). The universal distribution $p_{is}^*(x)$ (solid line) is the MC result of Tsypin and Blöte[22]. The scaling variable is $x = a_{\mathcal{M}}^{-1} L^{\beta/\nu}(\mathcal{M} - < \mathcal{M} >_c)$. Scale factors are chosen such that the distributions have unit variance.

FIG. 7. Density distribution p_L^ρ at the critical temperature $T_c^* = 0.04917$ and chemical potential μ^* determined such that $p_L(\mathcal{M})$ is symmetric for the volumes $V/\sigma^3 = 5000$ (open squares), 10000 (open circles), 20000 (solid squares) and 40000 (solid circles). The universal distribution $p_{is}^*(x)$ (dashed line) is the MC result of Tsypin and Blöte[22]. The scaling variable is $x = a_\rho^{-1} L^{\beta/\nu}(\rho - < \rho >)$. Scale factors are chosen such that the distributions have unit variance.

FIG. 8. Variation of $T_c^*(L)$ associated with the peak positions of the functions C_V, Y_3, Y_7, Y_{8-}, Y_{8+} and Y_{12}, defined in Ref. 15 along the locus $\chi_{NNN} = 0$ as a function of $L^{-1/\nu}$.

FIG. 9. The function $Y_7 = \frac{1}{V}[< O^2 > - < |O| >^2]$ with $O = N - < N >$ in the (T, ρ)-plane at volume $V/\sigma^3 = 5000$. The function is obtained from histogram reweighting using data given in Table I.

FIG. 10. Variation of the logarithm of the peak height of the saddle point in Y_7 as a function of $\ln L$.

FIG. 11. Variation of the total specific heat at constant volume C_V/V and the contribution from the chemical potential, C_μ/V, with temperature along the locus $\chi_{NNN} = 0$ at volumes V/σ^3=5000, 10000, 20000 and 40000.

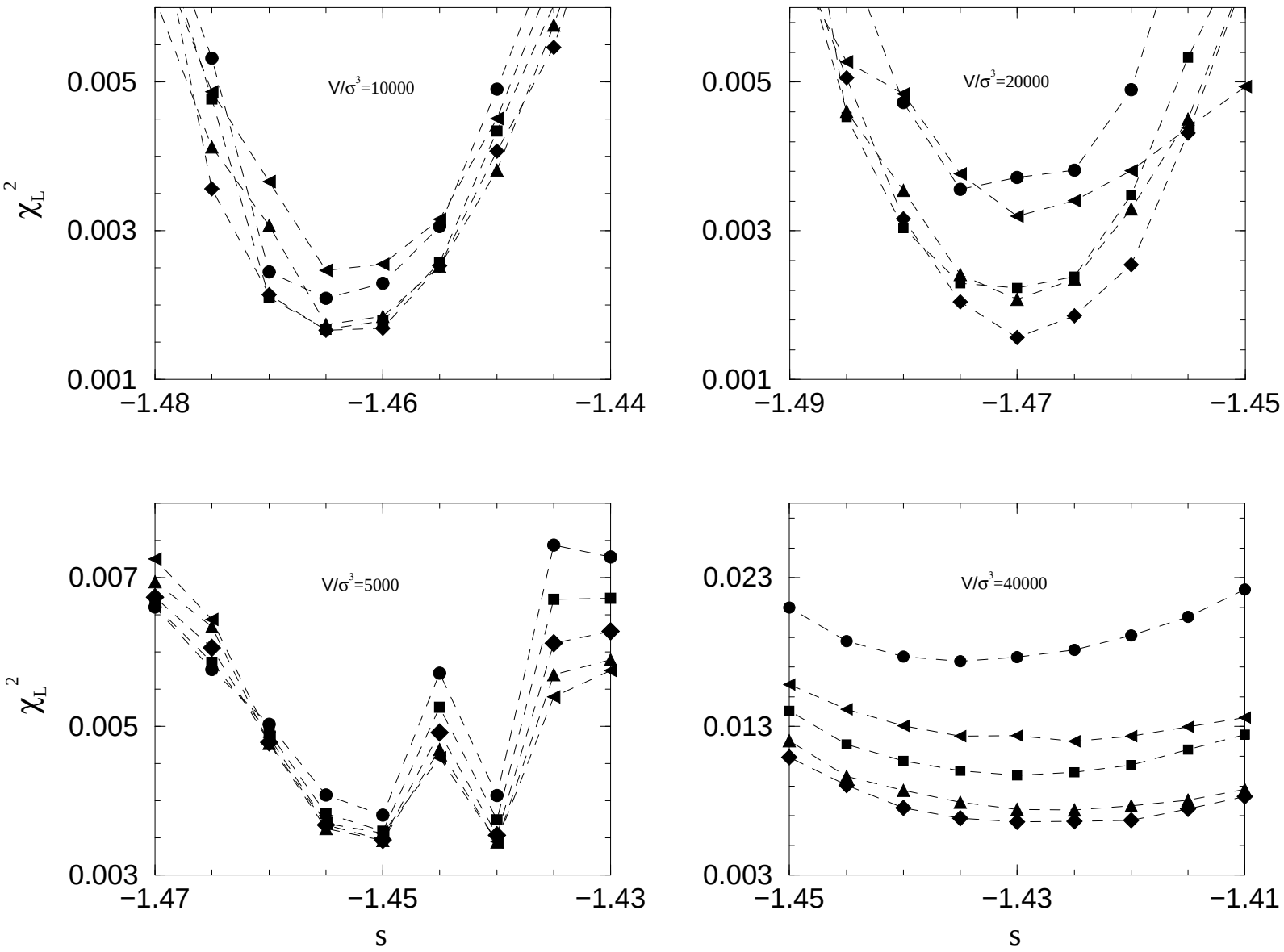
V/σ³=10000
V/σ³=20000
V/σ³=5000
V/σ³=40000
χ²L
s
0.001
0.003
0.005
0.007
0.013
0.023
−1.48
−1.46
−1.44
−1.49
−1.47
−1.45
−1.43
−1.41

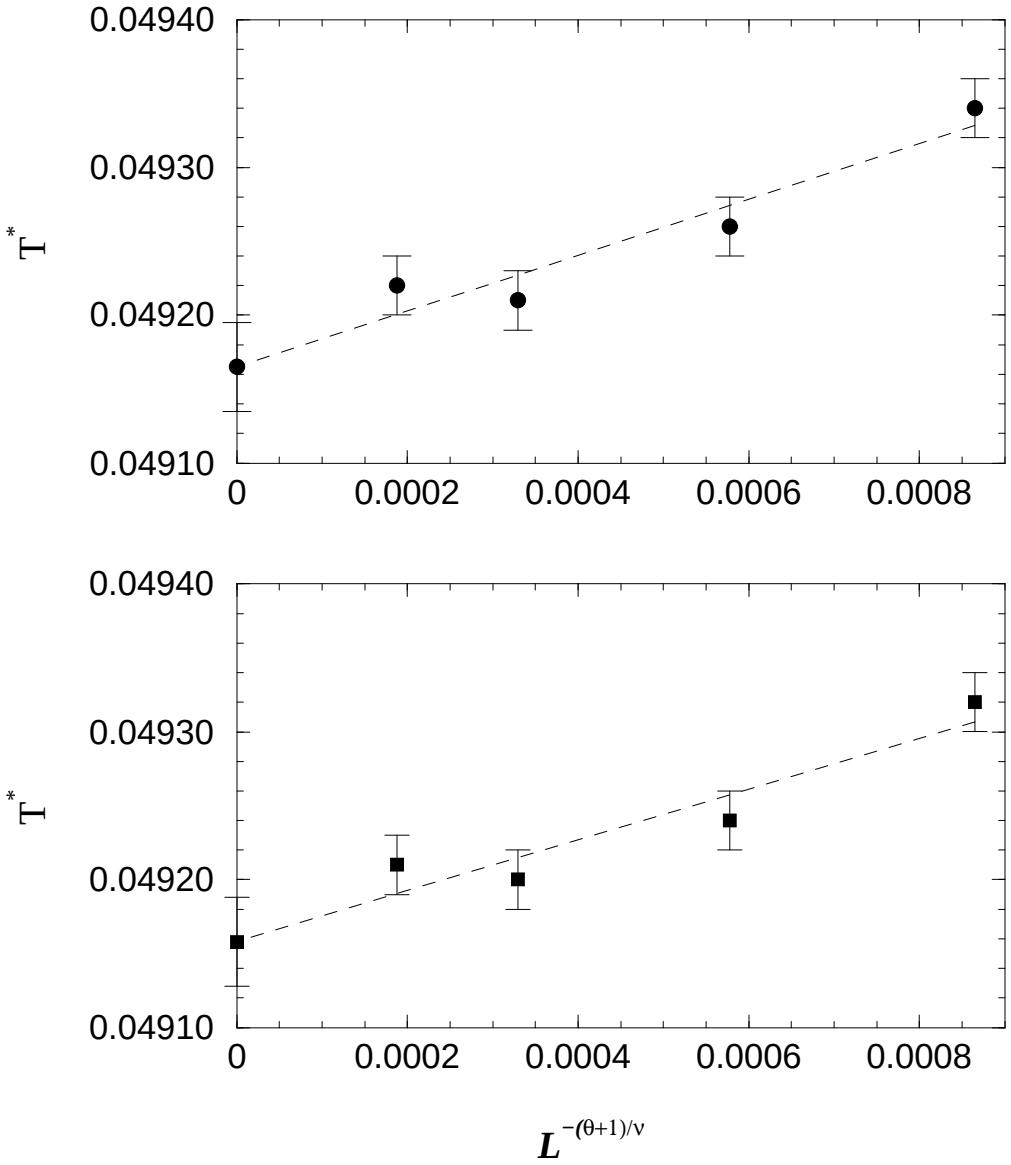
0.04940
0.04930
0.04920
0.04910
T*
0
0.0002
0.0004
0.0006
0.0008
0.04940
0.04930
0.04920
0.04910
T*
0
0.0002
0.0004
0.0006
0.0008
L^-(θ+1)/ν

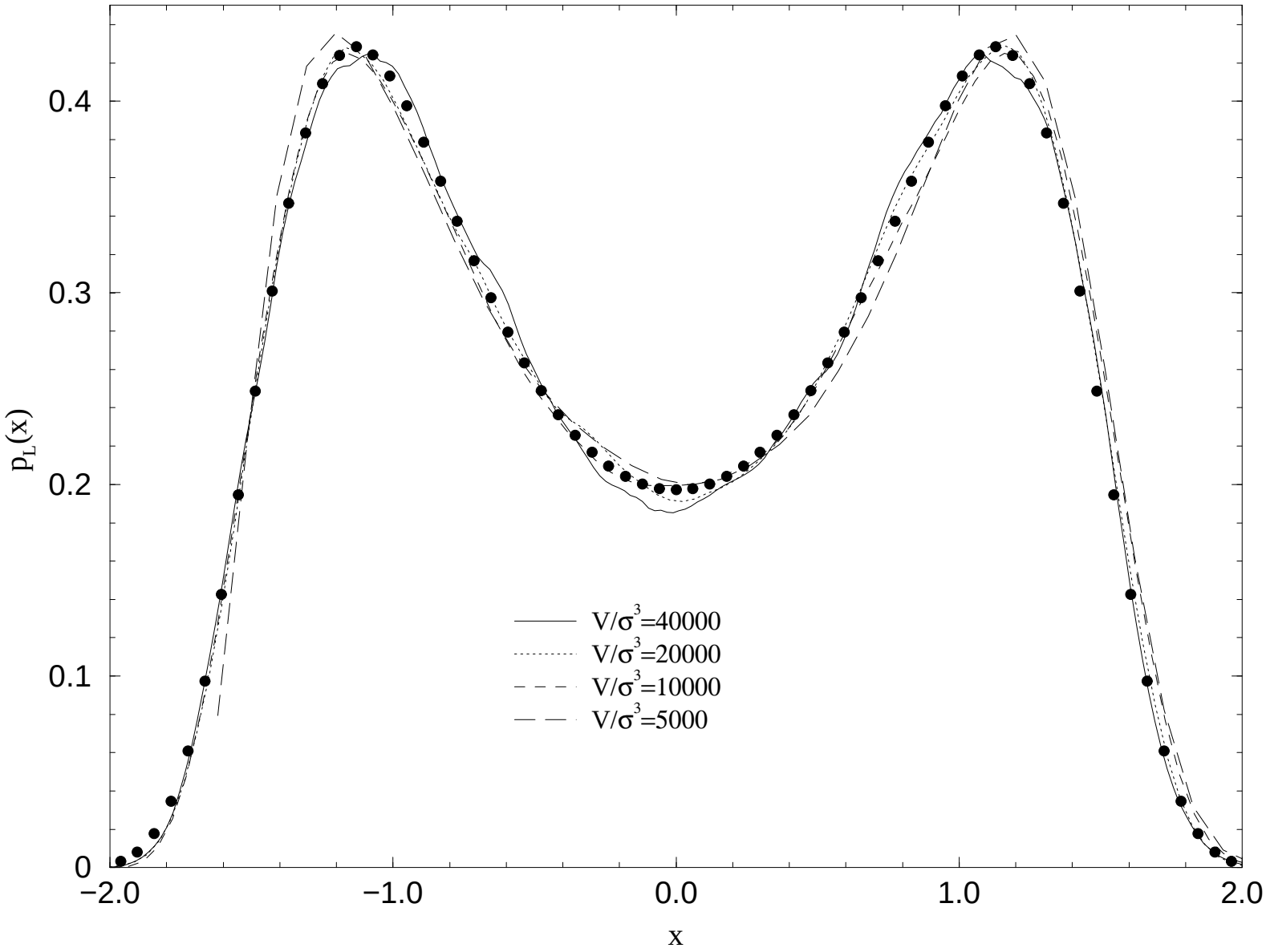
0.4
0.3
0.2
0.1
0
$p_L(x)$
−2.0
−1.0
0.0
1.0
2.0
x
V/σ^3=40000
V/σ^3=20000
V/σ^3=10000
V/σ^3=5000

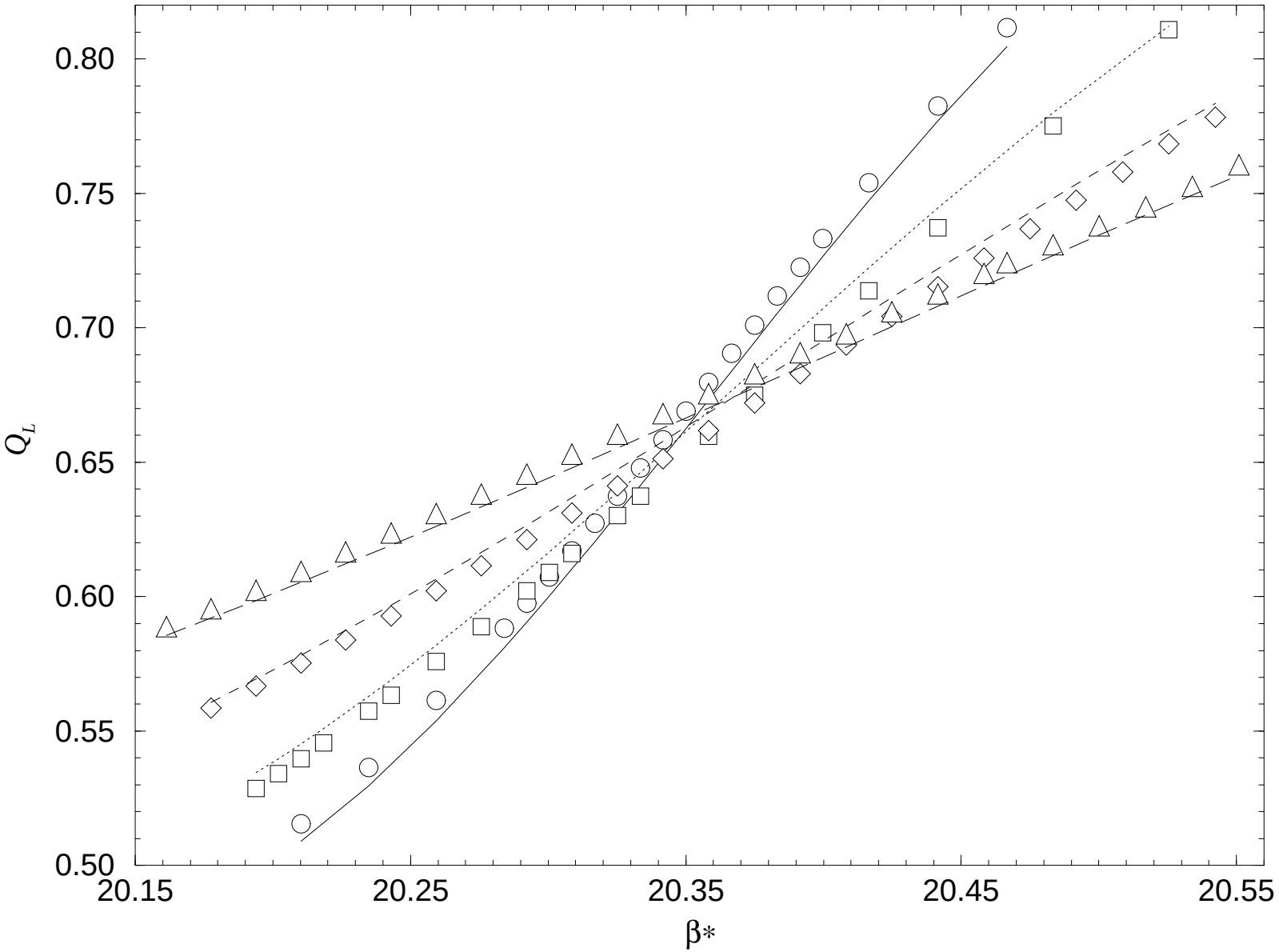
0.80
0.75
0.70
0.65
0.60
0.55
0.50
Q_L
20.15
20.25
20.35
20.45
20.55
β*

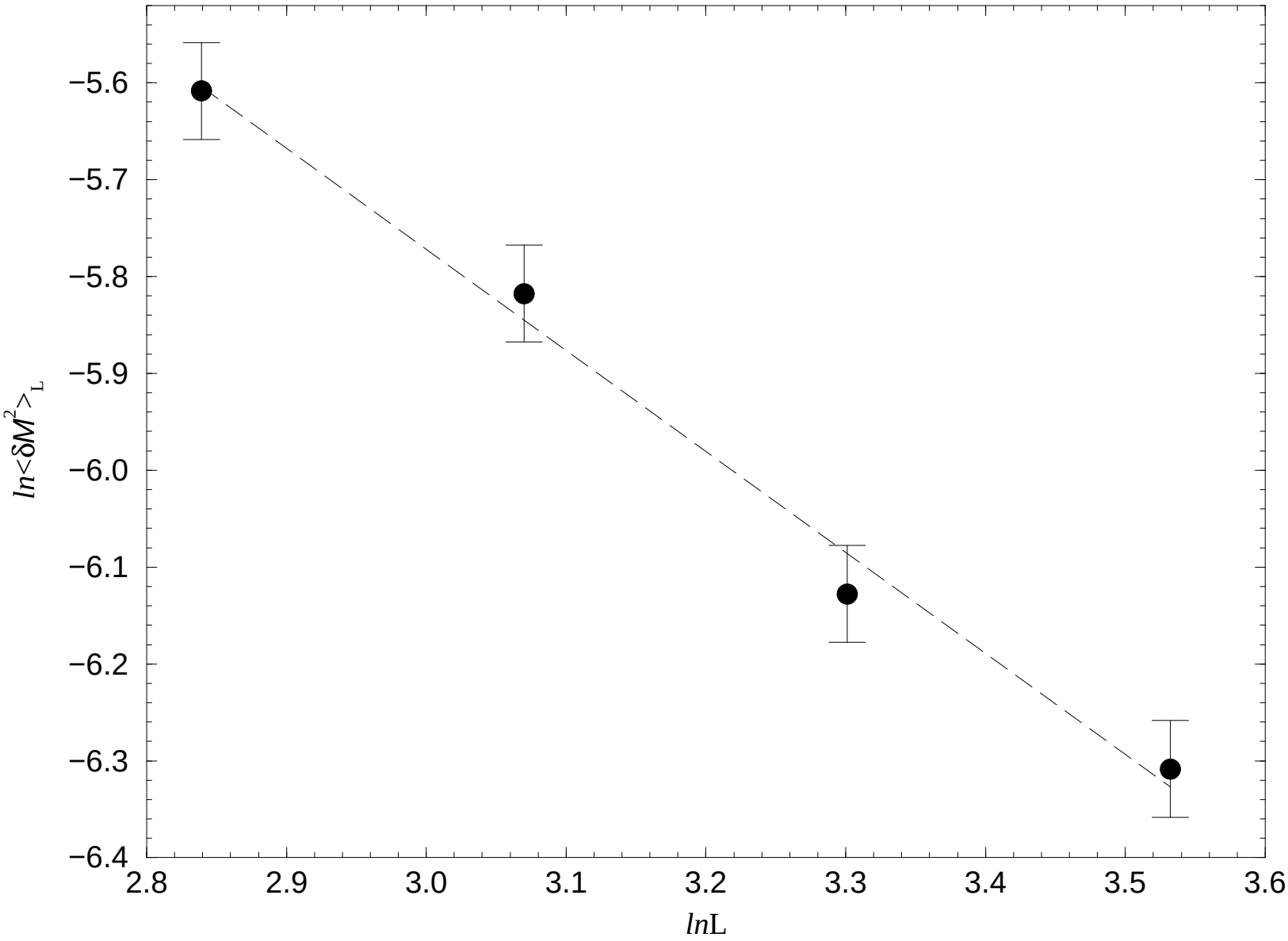
−5.6
−5.7
−5.8
−5.9
−6.0
−6.1
−6.2
−6.3
−6.4
2.8
2.9
3.0
3.1
3.2
3.3
3.4
3.5
3.6
ln<δM²>L
lnL

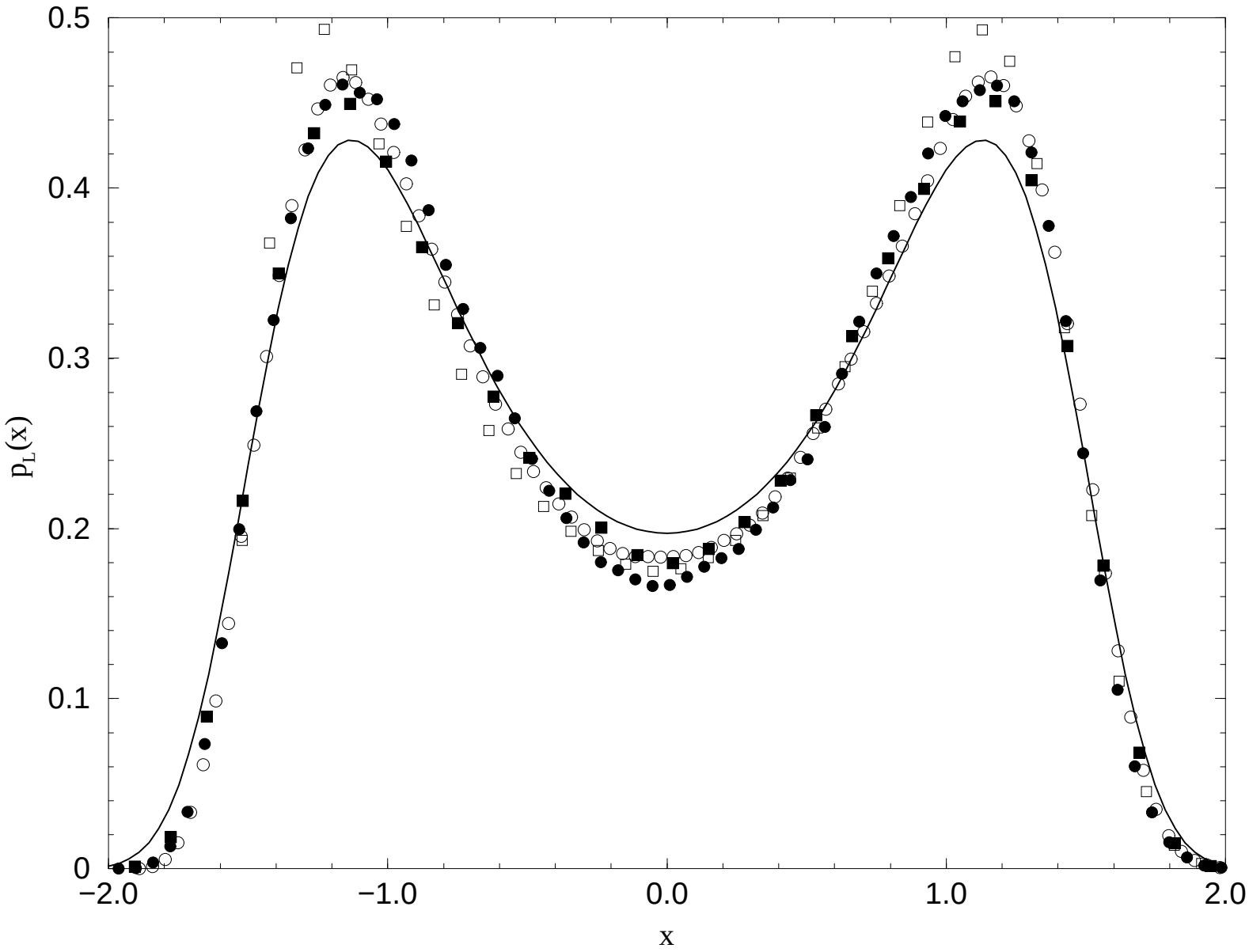
0.5
0.4
0.3
0.2
0.1
0
$p_L(x)$
−2.0
−1.0
0.0
1.0
2.0
x

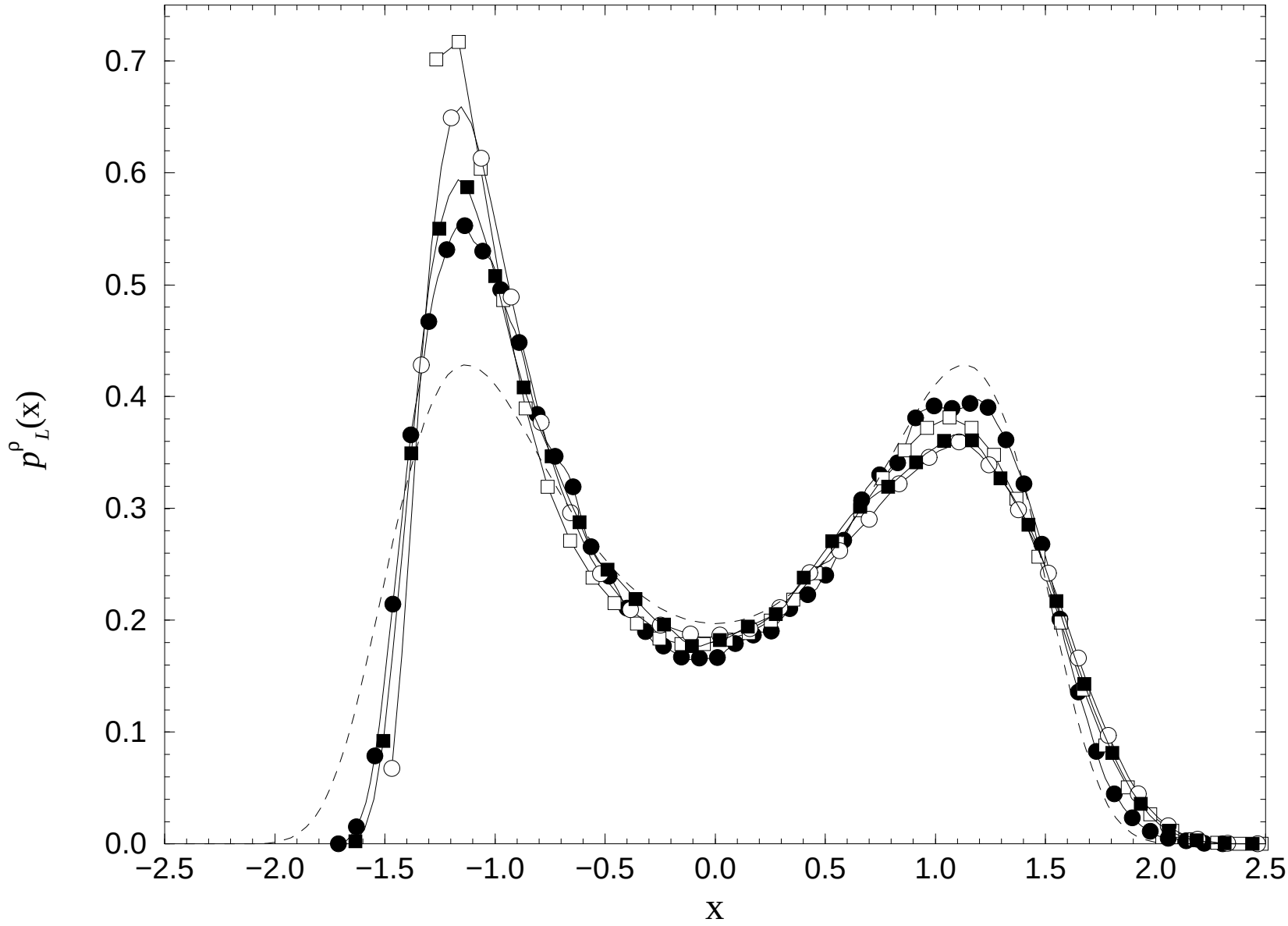
0.7
0.6
0.5
0.4
0.3
0.2
0.1
0.0
$p^{\rho}_{L}(x)$
−2.5
−2.0
−1.5
−1.0
−0.5
0.0
0.5
1.0
1.5
2.0
2.5
x

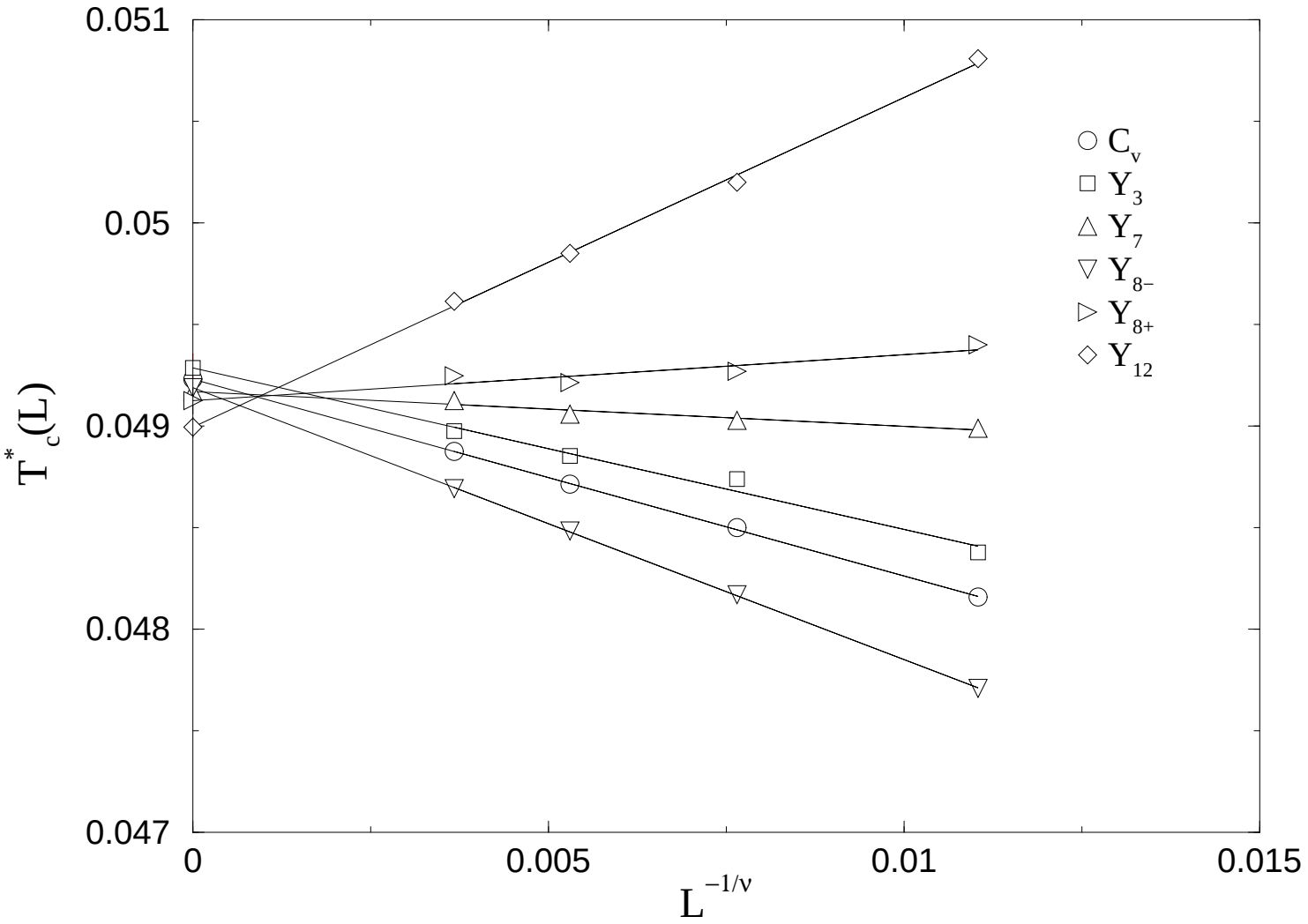
0.051
0.05
0.049
0.048
0.047
0
0.005
0.01
0.015
$T_c^*(L)$
$L^{-1/\nu}$
C_v
Y_3
Y_7
Y_{8-}
Y_{8+}
Y_{12}

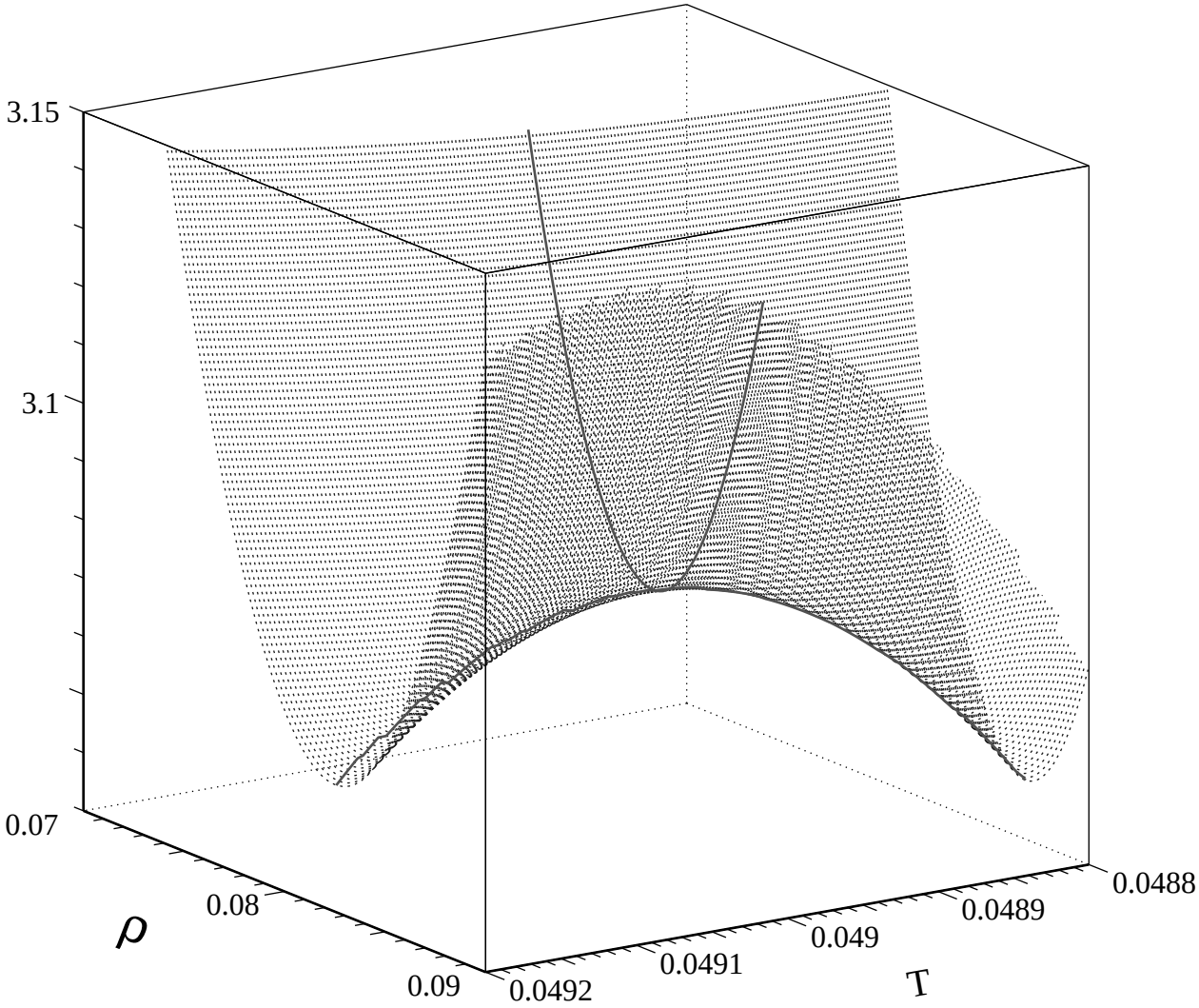
3.15
3.1
0.07
0.08
0.09
ρ
0.0492
0.0491
0.049
0.0489
0.0488
T

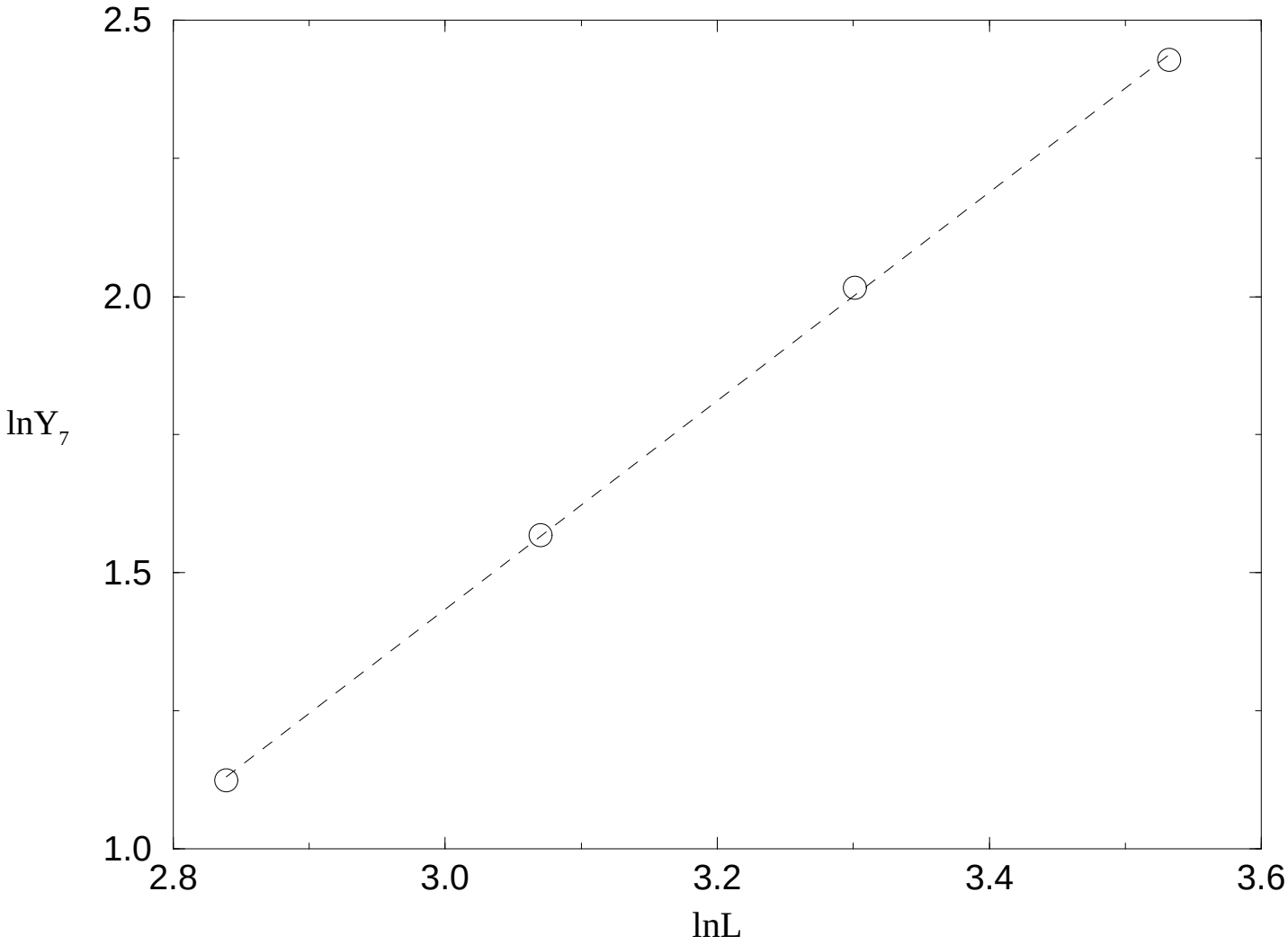
2.5
2.0
1.5
1.0
lnY7
2.8
3.0
3.2
3.4
3.6
lnL

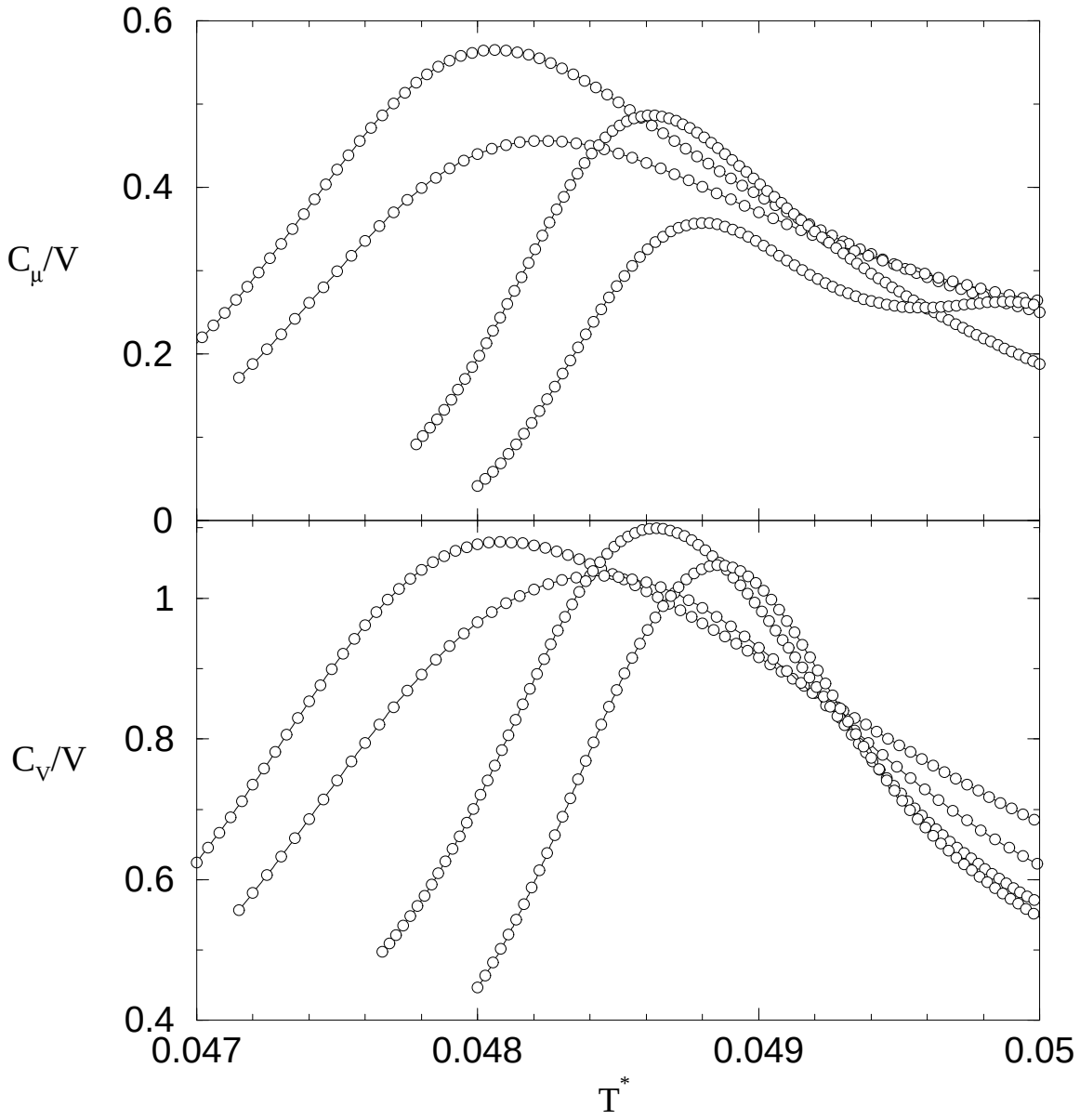
0.6
0.4
0.2
0
C_μ/V
1
0.8
0.6
0.4
C_V/V
0.047
0.048
0.049
0.05
T^*